Topological phase transitions in Graphene under periodic kicking

Tridev Mishra,[1,*] Anurag Pallaprolu,[1,†] Tapomoy Guha Sarkar,[1,‡] and Jayendra N. Bandyopadhyay[1,§]

[1] *Department of Physics, Birla Institute of Technology and Science, Pilani 333031, India.*

We consider a periodically δ-kicked Graphene system with the kicking applied in the $\hat{z}$ direction. This is known to open a gap at the Dirac points by breaking inversion symmetry through the introduction of a time-varying staggered sub-lattice potential. We look here at the topological properties of the gap closing-opening transition that occurs as functions of the driving amplitude. The dependence of the driving induced mass-term and the Berry curvature on the strength of driving is computed. The Chern number for the gapped-out points is computed numerically and its variation with the driving amplitude is studied. We observe that though the z-kicked Graphene system being time-reversal invariant remains topologically trivial in the bulk, it still permits a quantification of the topological changes that occur at individual gaps with changes in the sign of the mass term.

I. INTRODUCTION

Topology and notions intrinsic to it were introduced into the band theory of solids through the work of Thouless, Halperin and others[1–5] while theoretically exploring the remarkable phenomenon of the Quantum Hall Effect (QHE)[6,7]. These studies illuminated the role of integer valued topological invariants in uncovering the origins of robust quantization of such physical parameters as the Hall conductance and explaining the existence of conducting surface or edge states on bulk insulators. Many such exotic features were predicted and identified for other associated phenomena, which went beyond conventional time-reversal symmetry breaking, such as the Quantum Spin Hall Effect (QSHE), in graphene and other topological materials[8–11].Experimentally, this has sparked off a flurry of activity directed towards the synthesis of materials and nano structures which exhibit such novel features[12–17]. As such shaping the field of 'Topological Insulators'. From a theoretical perspective, the broad objective has been to achieve a comprehensive classification scheme for this phase of matter which relies on both, the dimensionality of their configuration space and the presence or absence of certain fundamental symmetries[18–20].

At the heart of these classification schemes lies the identification of certain topological invariants that correctly categorize the nature of topological order in the system. The Chern number[1,21], for example serves to quantify topological non-triviality, in terms of the number of gap-crossing, conducting boundary states. In principle, topological insulators with different Chern numbers belong to different topological phases and any interface between them will contain gap-closing edge states. Obtaining a non-trivial integer value for a topological invariant, for an isolated valence band of a system, is often realted to local singularities in the Berry curvature[22–25] at certain points over the system's toroidal Brillouin zone.

Graphene, beyond its much touted mechanical and transport properties[26–28], has shown itself to be rich in topological features. It is not exactly a bulk-insulator as it manifests semi-metallic, Dirac-like linear dispersion at low energies[29,30]. Besides, previously mentioned QSHE (in the presence of strong spin-orbit coupling), the manifestation of Zak phase and edge states in graphene ribbons has been studied[31], experimental validation of the QHE and Berry's phase for graphene has been peformed and various topological features of the honeycomb lattice have been investigated in cold-atom and photonic-crystal setups[32–36]. Studies of graphene irradiated or periodically driven by circularly polarized light have revealed rich topological textures beyond those seen in the undriven case[37–46]. An entire sub-domain of "Floquet Topological Insulators"[47] has emerged as a result, which has offered unprecedented control and freedom to engineer new topological phases and edge state(in some cases Majorana modes) behaviors[48–67] as well as a knob to study topological phase transitions in cold-atom or photonic crystal setups[68–74]. The theoretical classification of Floquet topological insulators and the identification of valid topological invariants that correctly characterize the bulk-edge correspondence for these systems is an on-going effort[75–81].

The use of circularly polarized light to drive graphene has the effect of breaking time reversal symmetry and opening up gaps in the Floquet band spectrum thereby generating a kind of photo-induced Hall effect[37]. An alternate means of periodic driving is the use of delta-function kicks, either single or double kicks, which has been widely studied in the contexts of quantum chaotic behavior, non-linear dynamics and localization-delocalization transitions, when applied to quantum top, rotor or Harper Hamiltonians[82–84]. This kind of kicking has also been shown to impart interesting topological properties in the form of new Floquet topological phases such as semi-metallic phases in Harper models[85], chiral edge modes in Quantum Hall systems[86], appearance of unexpected topological equivalence between spectrally distinct Hamiltonians[87] as well as generation of Majorana end modes in 1-D systems[88]. This has led to interest in studying Dirac systems especially graphene, its

* tridevmishra@pilani.bits-pilani.ac.in
† anurag.pallaprolu@gmail.com
‡ tapomoy1@gmail.com
§ jnbandyo@gmail.com

nano-ribbons and other hexagonal lattice models such as the Kitaev model under periodic driving or kicking.[89–91].

In this paper we study the topological aspects of graphene under the application of δ-function kicking. The obvious analytical advantages offered by such a driving protocol enable explicit calculations and reasonably approximate closed form expressions of the relevant topological quantities. The graphene Hamiltonian is considered under the tight binding and nearest neighbour approximations. The kicking protocol is selected to have the pseudo-spin structure of the Hamiltonian and is constructed using all three Pauli matrices along the lines of[91]. Likewise it is applied uniformly to each unit cell of the lattice. We look closely at the case of singly kicked graphene with kicking only along the σ_z component. The unitary time evolution operator over a period and hence the Floquet Hamiltonian is calculated. An interesting oscillatory variation of the mass term with the driving amplitude is noted, thus revealing how kicking modulates the gap as a function of the driving intensity. The mass term being a periodic, odd (in $[-\pi/2, \pi/2]$) function of the driving amplitude, changes sign indicating the existence of topologically distinct phases. A straight forward transformation of this term under time-reversal is used to show its symmetric nature. We focus our attention on the low energy spectrum in the vicinity of a single Dirac point of undriven graphene and fix this region of the Brillouin zone as the domain of our analytical calculations of the Berry curvature for the driven case. This simplifies calculations by allowing approximations for the form of spectrum and energy eigenvalues without compromising unduly on the quality of the topological information obtained for the said point in the Brillouin zone, where the gap opened due to driving, tames the singularities of the Berry flux to some extent and thus renders it calculable. The approximate analytic expression for the Berry curvature in this domain shows 'even' behaviour under a time-reversal transformation, however the globally calculated one is odd under such a transformation thus it is the breaking of inversion symmetry that causes a gap to open at the Dirac points. The z-kicking is thus shown to preserve time-reversal invariance of ordinary graphene.

In those instances where quantities, such as the Berry curvature, are required to be known over the entire Brillouin zone and hence necessitate a departure from low energy approximations, numerical methods have been used. The relevant topological measure for our case i.e. the Chern number is computed numerically by integration of the Berry curvature over the Brillouin zone region around a single source of Berry flux for a single valence band. The total Chern number for the valence band, for graphene under periodic kicking, evaluates to zero due to the driving-induced mass term having identical sign at both the Dirac nodes in the Brillouin zone. This is expected of the driving-generated 'Semenoff mass'[59] term causing the bulk to be a topologically-trivial insulating state. Though this may preclude the existence of edge states and any anomalous hall conductivity, valuable signatures for experimental detection, a local analysis may still be made of the gap closing-opening transition about an individual Dirac node as a function of the driving amplitude. We look at such transitions in the context of variations in Chern number as one modulates the strength of the drive. These are studied to illustrate the possibility of inducing controlled topological transitions in graphene. To round off our interest in the system we outline a few experimental scenarios, motivated by[91], that may replicate the topological phenomena described in our work.

II. FORMALISM

The contents of this paper rely on a tight-binding Hamiltonian under the nearest-neighbour approximation to describe graphene, to which the periodic kicking is applied as a train of δ-function pulses. We will also require the Berry curvature, formulated as an anti-symmetric tensor and computed using the notion of Bargmann invariants[25], to calculate the Chern numbers. In this section therefore, we address the requisite notation and mathematical machinery associated with these and proceed to the topological computations which are our final objective. We will also make use of some Floquet theory ideas, of an elementary nature, to develop the time independent Hamiltonian for graphene under periodic kicking.

A. Graphene under kicking

The kicked graphene system has recently been studied[91] in considerable detail as a platform for synthesizing novel dispersion relations and wave packet dynamics[91]. This work supplies the essential model which, in our study, serves as a prototype for interesting topological phenomena. Here, we shall reiterate the essential skeletal results of use to us and the reader is advised to look at the reference for details (expressions here borrows some of the notation from[91]).

The undriven graphene Hamiltonian is taken to be

$$\mathcal{H}(\mathbf{k}) = -\gamma \begin{bmatrix} 0 & 1 + e^{i\mathbf{k}.\mathbf{N}} + e^{i\mathbf{k}.\mathbf{N}'} \\ 1 + e^{-i\mathbf{k}.\mathbf{N}} + e^{-i\mathbf{k}.\mathbf{N}'} & 0 \end{bmatrix} \tag{1}$$

with $\mathbf{k} = (k_x, k_y)$ i.e reciprocal space coordinates and $\mathbf{N}$, $\mathbf{N}'$ being the lattice vectors to the nearest-neighbouring sites and γ the strength of the nearest-neighbor hopping. This admits more succinct expression in the language of Pauli matrices as

$$\mathcal{H}(\mathbf{k}) = -\gamma(G(\mathbf{k})\sigma^x - H(\mathbf{k})\sigma^y) \tag{2}$$

where, $G(\mathbf{k}) = 1 + \cos(\mathbf{k}.\mathbf{N}) + \cos(\mathbf{k}.\mathbf{N}')$ and $H(\mathbf{k}) = \sin(\mathbf{k}.\mathbf{N}) + \sin(\mathbf{k}.\mathbf{N}')$. The well known graphene eigenspectrum is readily described by $E(\mathbf{k}) =$

$\pm\gamma\sqrt{G(\mathbf{k})^2+H(\mathbf{k})^2}$,

$$E(\mathbf{k})=\pm\gamma\sqrt{3+2\cos(\sqrt{3}k_y a)+4\cos(\frac{\sqrt{3}k_y a}{2})\cos(\frac{3k_x a}{2})} \quad (3)$$

The kicking is applied as the following perturbing term to the Hamiltonian

$$\mathcal{H}_{kick,\mathbf{k}}(t)=(\alpha_x\sigma^x+\alpha_y\sigma^y+\alpha_z\sigma^z)\sum_{m=-\infty}^{m=\infty}\delta(t-mT) \quad (4)$$

and represents a general 2×2 kicking protocol with the $SU(2)$ pseudo-spin structure of the graphene Hamiltonian. The α_x,α_y and α_z stand for kicking amplitudes in the respective directions. Since we are consistently expressing the Hamiltonian and the perturbation to it in $\mathbf{k}$-space, the kicking is applied uniformly to every unit cell of graphene to have the reciprocal space representation of the above form. The dynamics of the system over a period T, under such a perturbation, are governed by an evolution operator $U_{XYZ}=U_{kick}U_{static}=e^{-i\boldsymbol{\alpha}.\boldsymbol{\sigma}}e^{-i\mathcal{H}(\mathbf{k})T}$ where, $U_{XYZ}=e^{-i\mathcal{H}_{XYZ}(\mathbf{k})T}$ with $\mathcal{H}_{XYZ}(\mathbf{k})$ as the Floquet Hamiltonian and, $\boldsymbol{\alpha}$ and $\boldsymbol{\sigma}$ are $(\alpha_x,\alpha_y,\alpha_z)$ and $(\sigma^x,\sigma^y,\sigma^z)$ respectively. Using the algebra of Pauli matrices and some standard results associated with them, it is possible (as illustrated in[91]) to obtain the exact form of $\mathcal{H}_{XYZ}(\mathbf{k})$. This is the model Hamiltonian which describes kicked graphene for our purposes and its eigenvalues are of the form

$$E_{\text{kick}}(\mathbf{k})=\mp\frac{1}{T}\arccos[\cos||\boldsymbol{\alpha}||\cos(E(\mathbf{k})T)+\frac{\gamma}{||\boldsymbol{\alpha}||E(\mathbf{k})}(\alpha_x G(\mathbf{k})-\alpha_y H(\mathbf{k}))\sin||\boldsymbol{\alpha}||\sin(E(\mathbf{k})T)] \quad (5)$$

where $||\boldsymbol{\alpha}||=\sqrt{\alpha_x^2+\alpha_y^2+\alpha_z^2}$. In particular, we are interested in a kicking scheme where $\alpha_z\neq 0$ while $\alpha_x=\alpha_y=0$ and henceforth assume these parameter values in the perturbing Hamiltonian in Eq.(4). This choice stems from our objective of using the kicking to open a gap and study this transition in a minimal model that would achieve it. This simplifies the eigenvalues to

$$\epsilon_Z(\mathbf{k})=\pm\frac{1}{T}\cos^{-1}(\cos(\alpha_z)\cos(E(\mathbf{k})T)). \quad (6)$$

This spectrum is gapped at the location of the Dirac points of unkicked graphene and shows a quadratic departure in this neighbourhood. Hence these are the eigenvalues of $\mathcal{H}_{XYZ}(\mathbf{k})$ with only $\alpha_z\neq 0$ which we shall denote $\mathcal{H}_Z(\mathbf{k})=\epsilon_z\boldsymbol{\sigma}.\hat{m}(\mathbf{k})$, where the form of $\hat{m}(\mathbf{k})$ can be read off from the structure of $\mathcal{H}_{XYZ}(\mathbf{k})$ after accounting for the z-driving. We will later on make some approximations to simplify the form of $\mathcal{H}_Z(\mathbf{k})$ for calculating an analytical approximant of the Berry curvature in the neighborhood of a kicking induced gap opening. Presently, we shall touch upon the Bargmann invariants and density matrices based approach to calculating the Berry curvature that shall form the backbone of those calculations.

B. Bargmann Invariants and Berry Curvature

A certain class of topological invariants for quantum systems are calculated using gauge and reparametrization invariant quantities defined over a parametrized space of the system's states. Thus, Chern numbers are computed from the Berry connection (gauge potential)[22] or post-Stokes' theorem, the Berry curvature, which is such a quantity defined over a complex projective ray space constructed from the system's Hilbert space. An elegant formalism that captures the topological character of the geometric phase, free from the constraints of adibaticity or cyclic evolution, is based on the use of Bargmann invariants[25]. These are in general complex valued invariants expressed in the Von Neumann density matrix formulation.

To put it briefly, let $U(1)$ invariant pure state density matrices $\rho=|\psi\rangle\langle\psi|$ denote physical states or rays in a complex projective ray space. Then, the Bargmann invariants, are products of these density matrices, $\rho_1\rho_2\cdots\rho_j$ with the j states forming the vertices of a j-sided polygon in ray space. In more explicit terms a Bargmann invariant of order j for a set of as many normalized states $|\psi_j\rangle$ such that $\langle\psi_j|\psi_{j+1}\rangle\neq 0$, is

$$\mathcal{B}^j(\psi_1,\cdots,\psi_j)=\langle\psi_1|\psi_2\rangle\langle\psi_2|\psi_3\rangle\cdots\langle\psi_{j-1}|\psi_j\rangle\langle\psi_j|\psi_1\rangle \quad (7)$$

with invariance under transformations belonging to $U(1)\times U(1)\times\cdots j\ times$. The integral of the ray space curvature tensor over the region enclosed by this polygon is the total flux of the Berry field through it and gives the geometric phase acquired by the state on travelling the closed circuit demarcated by the sides of the polygon. It is the phase of the Bargmann invariant for some path in ray space which holds the geometric phase information. The phase of the Bargmann invariant for an infinitesimal polygon of the kind in Eq.(7) is obtained as,

$$\mathcal{F}_{\alpha\beta}(\mathbf{x})=\frac{1}{2i}\text{Tr}(\rho(\mathbf{x})\big[\partial_\alpha\rho(\mathbf{x}),\partial_\beta\rho(\mathbf{x})\big]) \quad (8)$$

i.e. an antisymmetric tensor denoting a curvature 2-form, the Berry curvature or field. The $\mathbf{x}=(x_1,x_2,\cdots,x_{2N-2})$ denotes coordinates of points in ray space under some suitable parametrization, ray space being $2N-2$-dimensional for an N-level quantum system. In the case of lattice systems and Bloch functions these coordinates are $\mathbf{k}$-space coordinates $(k_x,k_y,\cdots)$. The indices α and β run over the ray space dimensions. It is interesting to note that one can recover the customary expression for the Berry curvature, over the Brillouin zone, for 2×2 systems with translational invariance of the kind $H(\mathbf{k})=\boldsymbol{\sigma}.\hat{n}(\mathbf{k})$, which is in general given by $\boldsymbol{\Omega}(\mathbf{k})=\frac{1}{2|\hat{n}(\mathbf{k})|^3}\hat{n}(\mathbf{k}).[\partial_{k_x}\hat{n}(\mathbf{k})\times\partial_{k_y}\hat{n}(\mathbf{k})]$ upon making the substitution $\rho(\mathbf{k})=\frac{1}{2}(1+\boldsymbol{\sigma}.\hat{n}(\mathbf{k}))$ in Eq.(8), $\mathbf{k}$ serving the role of $\mathbf{x}$. This is drawn from a general analogy to the spin-$\frac{1}{2}$ Bloch sphere construction for 2-level systems with Dirac structure. We use Eq.(8) with the same analogy for our z-kicked graphene Hamiltonian $\mathcal{H}_Z(\mathbf{k})=\epsilon_z\boldsymbol{\sigma}.\hat{m}(\mathbf{k})$

and in what follows perform an approximate analytical calculation of the Berry curvature for this system.

C. Berry Curvature and Chern numbers for graphene under z-kicking

Since we are interested in the gap opening at a Dirac point and the associated topology it helps to limit our domain to the region of the Brillouin zone near a single Dirac point, $\mathbf{K}$ or $\mathbf{K}'$ of graphene. As we keep the underlying $\mathbf{k}$-space reference the same, both for graphene with and without driving, the Dirac point and the gapped point are the same in terms of reciprocal space coordinates in the Brillouin zone. Thus the label of $\mathbf{K}$ or $\mathbf{K}'$ points is retained even post driving when a gap has appeared and one is not technically speaking of a Dirac-touching point. Also, this ensures the validity of certain approximations which considerably simplify calculations. The most significant among these being the linearity of the low-energy dispersion around the Dirac points for ordinary graphene. This permits one to use $G(k_x,k_y) = -\frac{3a}{2}k_y \quad H(k_x,k_y) = \frac{3a}{2}k_x$, where a is the lattice constant for graphene and for the spectrum this implies $E(k_x,k_y) = \frac{3\gamma}{2}\sqrt{k_x^2+k_y^2}$. These substitutions are made while determining the form of $\mathcal{H}_Z(\mathbf{k})$ in the manner outlined in section II A. This essentially involves computing the structure of the unit vector $\hat{m}(\mathbf{k})$. The exact form of $\hat{m}(\mathbf{k})$ is determined by using identities for products of exponentiated $SU(2)$ Hamiltonians as mentioned earlier and in detail in[91].We can exploit the fact that the z-kicked graphene dispersion, ϵ_z is quadratic to a first approximation near the gap. This allows one to simplify a term, of the form $\sin(\epsilon_z(\mathbf{k})T)$, occurring in the expression for $\hat{m}(\mathbf{k})$ with this quadratic approximation. Essentially, $\cos(\epsilon_z(\mathbf{k})T) = \cos(\alpha_z)\cos(E(\mathbf{k})T) \approx \cos(\alpha_z)(1-\frac{E(\mathbf{k})^2T^2}{2})$ which implies $\sin(\epsilon_z(\mathbf{k})T) \approx \sqrt{1-\cos^2(\alpha_z)(1-E(\mathbf{k})^2T^2)}$. Proceeding in this way we get an $\hat{m}(\mathbf{k})$ of the form

$$\begin{aligned}&\left[\frac{\gamma TG(\mathbf{k})\cos(\alpha_z)+\alpha_z\gamma TH(\mathbf{k})\sin(\alpha_z)}{\sqrt{1-\cos^2(\alpha_z)\big(1-E(\mathbf{k})^2T^2\big)}}\right]\hat{x}\\ &+\left[\frac{-\gamma TH(\mathbf{k})\cos(\alpha_z)+\alpha_z\gamma TG(\mathbf{k})\sin(\alpha_z)}{\sqrt{1-\cos^2(\alpha_z)(1-E(\mathbf{k})^2T^2)}}\right]\hat{y}\\ &+\left[\frac{-\sin(\alpha_z)(1-\frac{E(\mathbf{k})^2T^2}{2})}{\sqrt{1-\cos^2(\alpha_z)(1-E(\mathbf{k})^2T^2)}}\right]\hat{z}\end{aligned} \tag{9}$$

where one has to make the substitutions for $G(\mathbf{k})$ and $H(\mathbf{k})$ just discussed. In order to compute the Berry curvature for this system using Eq.(8) the required density matrix representation, as a function of $\mathbf{k}$-space coordinates, is given by $\rho_\pm(\mathbf{k}) = \frac{1}{2}(1 \pm \mathcal{H}_Z(\mathbf{k})/\epsilon_z(\mathbf{k}))$. A straight forward consequence of the analogy discussed towards the end of section II B. Thus one needs to consider Eq.(8) in terms of the Brillouin zone variables in the form $\mathcal{F}_{k_x,k_y}(\mathbf{k}) = \frac{1}{2i}\mathrm{Tr}(\rho(\mathbf{k})\big[\partial_{k_x}\rho(\mathbf{k}),\partial_{k_y}\rho(\mathbf{k})\big])$. The $\rho_+(\mathbf{k})$ and $\rho_-(\mathbf{k})$ denote the choice of density matrix for the conduction and valence bands respectively, at zero of temperature with the Fermi level assumed to be situated at the Dirac point. In the gap opened scenario it will lie in the gap exactly in the middle of the two bands.

The density matrices are therefore constituted of the matrix elements of $\mathcal{H}_Z(\mathbf{k})/\epsilon_z(\mathbf{k})$ which is basically the matrix $\boldsymbol{\sigma}.\hat{m}(\mathbf{k})$. Under the assumptions made previously, the non-trivial $(1,1)$ and $(1,2)$ terms of this matrix, are given by

$$(\boldsymbol{\sigma}.\hat{m}(\mathbf{k}))_{1,1} = \frac{-\sin\alpha_z\left(1-\frac{T^2\gamma^2 9a^2}{8}(k_x^2+k_y^2)\right)}{\sqrt{1-\left(1-\frac{T^2\gamma^2 9a^2}{4}(k_x^2+k_y^2)\cos^2\alpha_z\right)}} \tag{10}$$

$$\begin{aligned}(\boldsymbol{\sigma}.\hat{m}(\mathbf{k}))_{1,2} = &\frac{\frac{3a\gamma T}{2}(-k_y\cos\alpha_z+\alpha_z k_x\sin\alpha_z)}{\sqrt{1-\left(1-\frac{T^2\gamma^2 9a^2}{4}(k_x^2+k_y^2)\cos^2\alpha_z\right)}}\\ &+\frac{i\frac{3a\gamma T}{2}(k_x\cos\alpha_z+k_y\alpha_z\sin\alpha_z)}{\sqrt{1-\left(1-\frac{T^2\gamma^2 9a^2}{4}(k_x^2+k_y^2)\cos^2\alpha_z\right)}}\end{aligned} \tag{11}$$

This yields the following valence-band Berry curvature for z-kicked graphene, near a gap opening and subject to the approximations made,

$$\mathcal{F}_{k_x,k_y}(\mathbf{k}) = \frac{1}{2}\frac{\omega^4\sin(\alpha_z)(k_x^2+k_y^2)(\alpha_z^2\sin^2(\alpha_z)+\cos^2(\alpha_z))}{(1-[1-\omega^2(k_x^2+k_y^2)]\cos^2(\alpha_z))^{\frac{3}{2}}} \tag{12}$$

where $\omega = \frac{3a\gamma T}{2}$. This is computed around a $\mathbf{K}$ point and for a $\mathbf{K}'$ point is the same expression with its sign flipped. It is found to be in good agreement with a numerically calculated Berry curvature for the same domain obtained numerically. The expression illustrates the functional dependence of the Berry curvature on the amplitude of the driving, α_z. In the spirit of the approximations that have led to the above result one could venture to write the total Berry curvature function over the entirety of the Brillouin zone as the sum of the approximate results for the $\mathbf{K}$ and $\mathbf{K}'$ points as $\mathcal{F}^{\mathrm{net}}_{k_x,k_y}(\mathbf{k}) = \mathcal{F}^{\mathbf{K}}_{k_x,k_y}(\mathbf{k}) + \mathcal{F}^{\mathbf{K}'}_{k_x,k_y}(\mathbf{k})$.

The Chern number, it follows, is also a function of the driving amplitude. This is obtained from an integral of the Berry curvature over the entire Brillouin zone

$$\mathcal{C} = \int_{\mathrm{BZ}}\mathcal{F}_{k_x,k_y}(\mathbf{k})dk_x\wedge dk_y \tag{13}$$

In case of graphene, the Berry curvature or field has singularities at the Dirac points and is zero elsewhere over the Brillouin Zone. So contributions to the Chern integral accumulate as sudden jumps of π and $-\pi$ at these

points due to integration of delta functions describing the Berry field here. The net total over the whole Brillouin zone is zero. In our case of z-kicked graphene the gap opened at the Dirac points makes the Berry curvature a finite though highly peaked function, with an asymptotic spread around the gapped point that rapidly dies out away from it. This shall be graphically depicted and elaborated in the next section. The Chern integral in this case, for a single gapped node, has to be truncated over a suitable domain to gather the dominant contribution thereby making the results of the integration not exact integers. This and other aspects are discussed in the following section from the point of view of gaining more analytical and numerical insight into the nature of the gap opening transition and its control through modulated driving.

III. RESULTS AND DISCUSSION

The kicking scheme adopted in our work has been noted to open a gap in the spectrum of graphene. The nature of this gap opening is instrumental in deciding the topological features of the resulting system. In this sense it would be instuctive to look at the mass term that the driving generates, which can be read off from the structure of $\mathcal{H}_Z(\mathbf{k})$ and using Eq.(10) as

$$\Delta = 2\epsilon_z(\boldsymbol{\sigma}.\hat{m}(\mathbf{k}))_{1,1} = \frac{-2\epsilon_z \sin\alpha_z \left(1 - \frac{\omega^2}{2}(k_x^2 + k_y^2)\right)}{\sqrt{1 - \left(1 - \omega^2(k_x^2 + k_y^2)\cos^2\alpha_z\right)}} \tag{14}$$

This term has a $m\sigma^z$ i.e. a Semenoff structure and hence results in the same sign for the mass term or gap at the two Dirac nodes $\mathbf{K}$ and $\mathbf{K}'$, a result of broken inversion symmetry due to a staggered sublattice potential at the A and B lattice sites of graphene. As a consequence, the Berry curvature takes on opposite signs at these points making the global Chern number over the entire Brillouin zone zero. This is in contrast to a Haldane term $m\sigma^z\tau^z$ which keeps both gaps of different signs ensuring a non-zero value for the global Chern number, where τ^z is the valley degree of freedom. This is usually found to occur for systems without time-reversal invariance. Such non-trivial insulating phases have been calculated for semi-Dirac materials driven using circularly-polarized light[59] and in half semi-metals with spin-orbit coupling[92,93]. Though topologically-trivial as a whole the z-kicked graphene system nevertheless exhibits locally, at each Dirac node, a driving modulated gap opening-closing transition. The $\sin\alpha_z$ term in the above equation determines the overall sign of the mass term and is itself a function of the driving, with change of sign in $\alpha_z \in [-(2n+1)\pi/2, (2n+1)\pi/2]$. Thus varying α_z it is possible to use the kicking to tune a topological transition locally at the $\mathbf{K}$ and $\mathbf{K}'$ points in the Brilloun zone.

This is illustrated in fig.(1) with a plot of the valence-band Berry curvature or field over a portion of reciprocal space equivalent to thrice the Brillouin zone of the system. This, though informationally redundant, helps to visualize the hexagonal pattern of the Berry curvature peaks and valleys over three pairs of $\mathbf{K}$ and $\mathbf{K}'$ points. Looking at either of the plots, which have been generated from a numerical calculation of $\mathcal{F}_{k_x,k_y}(\mathbf{k})$, it is easy to see that $\mathcal{F}_{k_x,k_y}(\mathbf{k})$ changes sign from a $\mathbf{K}$ to a $\mathbf{K}'$ point. The truncation in the peaks is a numerical cut-off as the values exceed numerical bounds rapidly, at the chosen α_z value. This is indicative of the sharply peaked bell-shaped structure of $\mathcal{F}_{k_x,k_y}(\mathbf{k})$ as is evident in its form in Eq.(12). This expression though a local approximation is found to be in close agreement with the numerically computed plot when examined in its domain of applicability, i.e. the neighbourhood of a Dirac point. Thereby lending credence to our approximation.

Further, since the two plots (a) and (b) look at $\mathcal{F}_{k_x,k_y}(\mathbf{k})$ behaviour for two α_z values of magnitude $\sqrt{3}$ but opposite signs, one is able to clearly distinguish that the system resides in distinct topological phases for these values of the driving amplitude. The fact that the peaks and valleys of $\mathcal{F}_{k_x,k_y}(\mathbf{k})$ undergo an inversion on going between the two plots attests to this local topological alteration of the gap at each node. From an analytical perspective, this might be argued on the grounds of the mass term Δ, see Eq.(14), undergoing a change in sign for the two α_z values considered. Thus, it is justified to regard the kicking scheme as an initiator of local topological transitions.

The broad overall dependence of $\mathcal{F}_{k_x,k_y}(\mathbf{k})$ and Δ on the driving is of an oscillatory-sinusoidal kind. This is exactly so for the mass term Δ and somewhat more complex with a quadratic modulation for $\mathcal{F}_{k_x,k_y}(\mathbf{k})$, see Eq.(12). Indeed there exists a clear correlation between the occurrence of sign flips in Δ and corresponding inversions in $\mathcal{F}_{k_x,k_y}(\mathbf{k})$ as one varies α_z. These reversals occur periodically leading to periodically recurring gap opening-closing transitions. As far as the range of the driving amplitude is concerned, we have restricted ourselves to $\alpha_z \in [-(2n+1)\pi/2, (2n+1)\pi/2]$, wherein our analyses apply perturbatively, i.e. without drastically altering the features expected of the band structure and the Brillouin zone (for instance location of $\mathbf{K}$ and $\mathbf{K}'$ points or equivalently gap openings). In cases where α_z values approach odd multiples of π the $\mathbf{K}$ and $\mathbf{K}'$ points undergo a shift akin to a rotation of the hexagon of Dirac nodes in reciprocal space. Thus $\mathcal{F}_{k_x,k_y}(\mathbf{k})$ has dominant contributions from $\mathbf{k}$-space points other than those involved previously. The behaviour can still be described in terms of the framework discussed here and one expects the trends to be inverted from those discussed above. So to speak an interchange of valence and conduction band $\mathcal{F}_{k_x,k_y}(\mathbf{k})$ behaviors, and also in the Chern number variation, which we now consider.

The Chern numbers for z-kicked graphene, with the Fermi level assumed to lie in the gap at zero temperature, can be calculated using the Eq.(13) supplied with the valence-band Berry curvature of Eq.(12). We per-

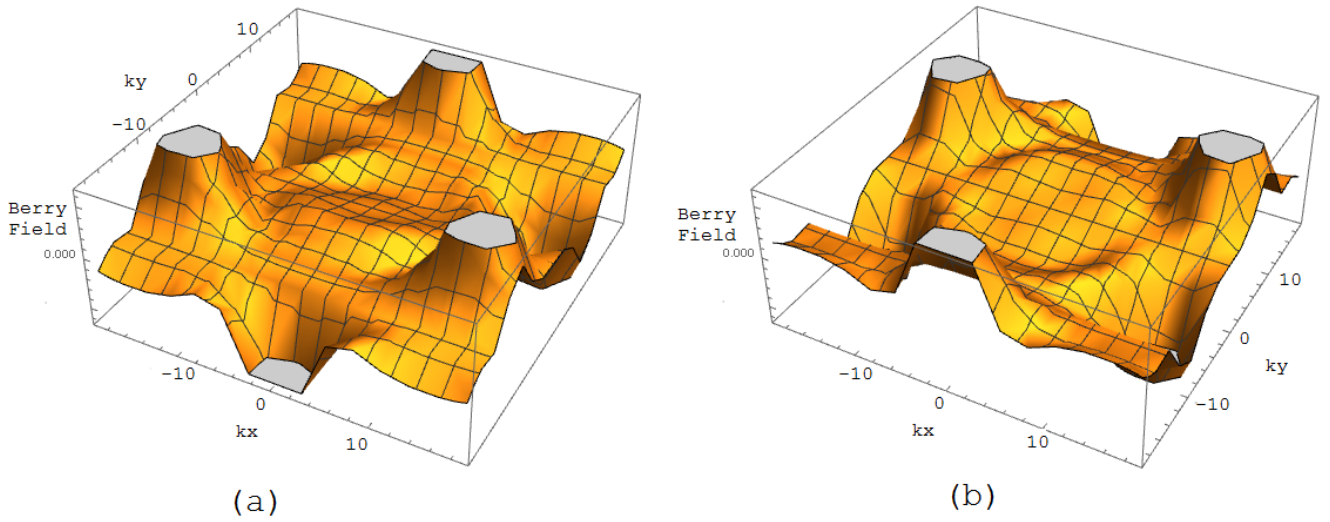

FIG. 1. The Berry curvature over a reciprocal space region of $(-6\pi, 6\pi) \times (-6\pi, 6\pi)$ for two values of α_z identical in magnitude but of opposite sign . Plot (a) is for $\alpha_z = \sqrt{3}$ and plot (b) for $\alpha_z = -\sqrt{3}$. γT is assumed to be 1. Notice the three prominent peaks and the three prominent valleys occurring in a hexagonal pattern. The peaks and valleys are exactly inverted on going from plot (a) to (b) and vice-versa. This indicates the local topological transition with change in α_z.

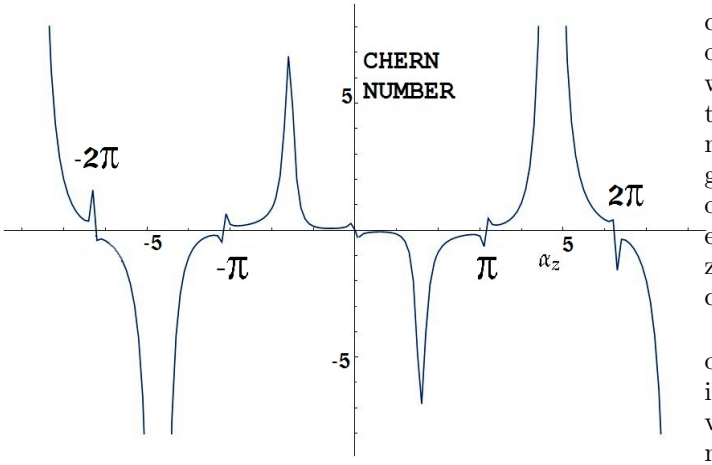

FIG. 2. The variation of the Chern number with α_z, near a **K** point.

form this integral numerically for the region around a single gap. The integral over the entire Brillouin zone is bound to be zero but for a given **K** (or **K′**) point a finite value is expected and found. As we are interested in the dependence of the Chern numbers on different values of driving amplitude we illustrate this variation in fig.2 .

As mentioned earlier, the peaked form of $\mathcal{F}_{k_x,k_y}(\mathbf{k})$ dictates that its value will fall off rapidly to zero away from the gap, but in an asymptotic fashion. Therefore, for our numerical integration, we define a rough cut-off in the Brillouin zone to calculate the Chern number. This is done by performing the integral in polar coordinates and choosing a radial limit beyond which $\mathcal{F}_{k_x,k_y}(\mathbf{k}) \approx 0^+$ or 0^- (upto 0 of the machine precision), depending on whether one is looking at a positive or negative peak of the Berry curvature. It is then not reasonable to demand that the Chern number evaluate to an exact integer and this deviation from some exact integer multiple of $\pm\pi$ is well documented in the case of anomalous Hall effect calculations for 2-D systems such as wurtzite and zinc blende quantum wells in the presence of spin orbit coupling[94].

The Chern number, as a continuous function of the driving amplitude α_z shown in fig.2, nonetheless crosses integer values for certain α_z values in the course of its variation. The important trends are observed at odd multiples of $\pi/2$ and integer multiples of π. At odd multiples of $\pi/2$ the Chern number is observed to assume its peak value and one sees the formation of a cusp with a reversal in the trend of its variation. An interesting association may be made here to the findings in[91] where they conclusively report the occurrence of dynamical localization of wavepackets for $\alpha_z = \pi/2$. The band structure at this driving is flat and **k** independent. Thus under these circumstances the Chern number takes on its peak values for the particular local driving regime. The absolute peak strengths of course increase with increase in the absolute value of α_z as is clear from the expression for $\mathcal{F}_{k_x,k_y}(\mathbf{k})$ in Eq.(12) where one notes the α_z^2 dependence. The sharp turn in the Chern number at a $\pi/2$ point is a signature of the trend reversal spoken of earlier for α_z lying outside of $[-(2n+1)\pi/2, (2n+1)\pi/2]$. The other feature of interest is the Chern numbers going to zero at integer multiples of π, a reflection of the flatness in

the Berry curvature at the considered portion of reciprocal space, which follows from the valence and conduction bands being repulsively curved away from one another. This is the regime where gap points have shifted to rotated positions and what was correctly assumed to be the source of the Berry field in the $[-(2n+1)\pi/2, (2n+1)\pi/2]$ regime of driving is no longer so. It will be necessary to change to a new Brillouin zone tilted wrt to the previous one and the right $\mathcal{F}_{k_x,k_y}(\mathbf{k})$ calculations need to be performed at these new $\widetilde{\mathbf{K}}$ and $\widetilde{\mathbf{K}}'$ points, rotated wrt the earlier $\mathbf{K}$ and $\mathbf{K}'$ points. A point worth keeping in mind here would be that experimentally atleast, the issue of taking the driving amplitude to arbitrarily large values is not without constraint and could lead to a greater influence of non-equilibrium affects not accounted for in our treatment. It would be advisable to regard the discussion here well within a $[-\pi/2, \pi/2]$ interval of the driving or a yet smaller one.

The expression for the Berry curvature obtained in Eq.(12) also offers insight into the nature of symmetries for the z-kicked graphene system. This is especially true for the time-reversal symmetry which protects the semimetallic Dirac point in graphene. It is known that for systems where time-reversal invariance is present the Berry curvature is an odd $\mathbf{k}$-space function under a time-reversal transformation i.e. $\mathcal{F}_{k_x,k_y}(-\mathbf{k}) = -\mathcal{F}_{k_x,k_y}(\mathbf{k})$, a common feature of spin-$\frac{1}{2}$ systems with translational invariance. Although, in our case, as far as the expression in Eq.(12) is concerned, this is not true and $\mathcal{F}_{k_x,k_y}(\mathbf{k})$ is not asymmetric either in k_x or k_y, still the numerically obtained global Berry curvature shows the odd behaviour (as seen in fig.1) expected of time-reversal invariant systems . Thus it is the broken inversion symmetry of graphene under an application of our z-kicking scheme, leading to the appearance of a gap. A time-reversal transformation of the mass term Δ also leaves it unchanged.

In our work, the entire discussion has been confined to a single gap opening and its topology precisely because the z-kicked graphene model studied here does not result in a non-zero global Chern number for the valence band. This leads to the bulk being topologically trivial though non-trivial topological behaviour does occur at individual gaps. A model that we believe would possess a finite non-zero global Chern number in addition to showing the kind of transitions studied here is the Haldane model of a hexagonal lattice with broken time-reversal symmetry with a kicking scheme applied to it. Such a system is expected to exhibit further interesting topological features and an enriched topological phase plot where one could find regions of different Chern numbers which would now also be functions of the driving amplitude. We plan to address this as an independent study in the future.

IV. EXPERIMENTAL ASPECTS

Before concluding we would like to mention a few systems where the phenomena detailed in our work have some possibility of occurring. We are guided in this by the proposals put forward in[91]. The one in particular involving kicking in the σ^z component is of relevance to our model. This involves placing a sample of hexagonal boron nitride over a layer of graphene in such a way that adjacent boron and nitrogen atoms are positioned over neighbouring carbon atoms of graphene[95–97]. Such a structural arrangement is permitted by the almost identical lattice constants of both materials. This proposal of[91] is motivated by its capacity to realize an effective sublattice potential for the underlying graphene layer.

Once this configuration is established the driving is implemented by applying periodically varying pressure on the two layers such that the distance between them varies periodically in time. This would effectively vary the sublattice potential experienced by the carbon atoms belonging to the A and B sublattices of graphene and thus produce the effects of z-kicking. In addition to the challenges posed by the requirements of high frequency driving, discussed in[91], the appearance of significant non-equilibrium effects in the system and the role of interactions becoming influential in the flat band regime of driving are additional features to contend with as the the strength of the driving is increased.

V. CONCLUSION

The z-directional periodic δ-kicking scheme applied to monolayer graphene generates a gap at the Dirac points by breaking the inversion symmetry of the system. The "Semenoff" mass-term that this generates in the Hamiltonian is observed to have a sinusoidal dependence on the driving amplitude. Thus giving rise to the possibility of tuning a gap closing-opening transition at the site of each Dirac node using the driving. This is indeed observed to be the case as seen from calculations of the Berry curvature and Chern numbers. The Berry curvature calculated analytically under local approximations close to a gap and that obtained numerically for the entire Brillouin zone agree in the appropriate limit. The principal range of the driving amplitude α_z lies $\in [-\pi/2, \pi/2]$ over which the system exhibits unique Chern number variation. Though topologically trivial globally due to time-reversal invariance the kicked system has local topological features at the gap-openings with the appearance of non-singular Berry curvature at these points in the Brillouin zone. Thus Chern numbers calculated around the gapped-out Dirac points transition continuously through non-integer values also, as the driving strength is modulated.

VI. ACKNOWLEDGEMENTS

T.M. would like to acknowledge discussions with Prof. Diptiman Sen and Dr. Utso Bhattacharya in meetings at ICTS. A.P. would like to thank Dr. Adhip Agarwala for

valuable inputs. T.G.S and J.N.B would like to thank Prof. N. Mukunda for providing his lecture notes on various aspects of geometric phase.

[1] D. J. Thouless, M. Kohmoto, M. P. Nightingale, and M. den Nijs, Phys. Rev. Lett. **49**, 405 (1982).
[2] B. I. Halperin, Phys. Rev. B **25**, 2185 (1982).
[3] J. E. Avron, R. Seiler, and B. Simon, Phys. Rev. Lett. **51**, 51 (1983).
[4] Q. Niu, D. J. Thouless, and Y.-S. Wu, Phys. Rev. B **31**, 3372 (1985).
[5] Y. Hatsugai, Phys. Rev. Lett. **71**, 3697 (1993).
[6] K. v. Klitzing, G. Dorda, and M. Pepper, Phys. Rev. Lett. **45**, 494 (1980).
[7] R. B. Laughlin, Phys. Rev. B **23**, 5632 (1981).
[8] B. A. Bernevig and S.-C. Zhang, Phys. Rev. Lett. **96**, 106802 (2006).
[9] B. A. Bernevig, T. L. Hughes, and S.-C. Zhang, Science **314**, 1757 (2006), http://science.sciencemag.org/content/314/5806/1757.full.pdf.
[10] C. L. Kane and E. J. Mele, Phys. Rev. Lett. **95**, 226801 (2005).
[11] C. Kane and E. Mele, Phys. Rev. Lett. **95**, 146802 (2005).
[12] L. Fu, C. L. Kane, and E. J. Mele, Phys. Rev. Lett. **98**, 106803 (2007).
[13] J. E. Moore, Nature **464**, 194 (2010).
[14] Y. Chen, J. Analytis, J.-H. Chu, Z. Liu, S.-K. Mo, X.-L. Qi, H. Zhang, D. Lu, X. Dai, Z. Fang, et al., Science **325**, 178 (2009).
[15] M. Z. Hasan, S.-Y. Xu, D. Hsieh, L. A. Wray, and Y. Xia, arXiv preprint arXiv:1401.0848 (2014).
[16] M. Z. Hasan and C. L. Kane, Rev. Mod. Phys. **82**, 3045 (2010).
[17] X.-L. Qi and S.-C. Zhang, Rev. Mod. Phys. **83**, 1057 (2011).
[18] A. Altland and M. R. Zirnbauer, Phys. Rev. B **55**, 1142 (1997).
[19] A. P. Schnyder, S. Ryu, A. Furusaki, and A. W. W. Ludwig, Phys. Rev. B **78**, 195125 (2008).
[20] A. Kitaev, in AIP Conference Proceedings, Vol. 1134 (2009).
[21] M. Kohmoto, Annals of Physics **160**, 343 (1985).
[22] M. V. Berry, Proceedings of the Royal Society of London A: Mathematical, Physical and Engineering Sciences **392**, 45 (1984), http://rspa.royalsocietypublishing.org/content/392/1802/45.full.pdf.
[23] N. Mukunda and R. Simon, Annals of Physics **228**, 205 (1993).
[24] N. Mukunda and R. Simon, Annals of Physics **228**, 269 (1993).
[25] E. M. Rabei, Arvind, N. Mukunda, and R. Simon, Phys. Rev. A **60**, 3397 (1999).
[26] A. H. Castro Neto, F. Guinea, N. M. R. Peres, K. S. Novoselov, and A. K. Geim, Rev. Mod. Phys. **81**, 109 (2009).
[27] S. Das Sarma, S. Adam, E. H. Hwang, and E. Rossi, Rev. Mod. Phys. **83**, 407 (2011).
[28] M. O. Goerbig, Rev. Mod. Phys. **83**, 1193 (2011).
[29] F. D. M. Haldane, Phys. Rev. Lett. **61**, 2015 (1988).
[30] Y. Hatsugai, T. Fukui, and H. Aoki, Phys. Rev. B **74**, 205414 (2006).
[31] P. Delplace, D. Ullmo, and G. Montambaux, Phys. Rev. B **84**, 195452 (2011).
[32] Y. Zhang, Y.-W. Tan, H. L. Stormer, and P. Kim, Nature **438**, 201 (2005).
[33] S. Koghee, L.-K. Lim, M. O. Goerbig, and C. M. Smith, Phys. Rev. A **85**, 023637 (2012).
[34] L. Tarruell, D. Greif, T. Uehlinger, G. Jotzu, and T. Esslinger, Nature **483**, 302 (2012).
[35] M. C. Rechtsman, Y. Plotnik, J. M. Zeuner, D. Song, Z. Chen, A. Szameit, and M. Segev, Phys. Rev. Lett. **111**, 103901 (2013).
[36] G. Jotzu, M. Messer, R. Desbuquois, M. Lebrat, T. Uehlinger, D. Greif, and T. Esslinger, Nature **515**, 237 (2014).
[37] T. Oka and H. Aoki, Phys. Rev. B **79**, 081406 (2009).
[38] T. Kitagawa, T. Oka, A. Brataas, L. Fu, and E. Demler, Phys. Rev. B **84**, 235108 (2011).
[39] Z. Gu, H. A. Fertig, D. P. Arovas, and A. Auerbach, Phys. Rev. Lett. **107**, 216601 (2011).
[40] E. Suárez Morell and L. E. F. Foa Torres, Phys. Rev. B **86**, 125449 (2012).
[41] T. Iadecola, D. Campbell, C. Chamon, C.-Y. Hou, R. Jackiw, S.-Y. Pi, and S. V. Kusminskiy, Phys. Rev. Lett. **110**, 176603 (2013).
[42] P. Delplace, A. Gómez-León, and G. Platero, Phys. Rev. B **88**, 245422 (2013).
[43] P. M. Perez-Piskunow, G. Usaj, C. A. Balseiro, and L. E. F. F. Torres, Phys. Rev. B **89**, 121401 (2014).
[44] G. Usaj, P. M. Perez-Piskunow, L. E. F. Foa Torres, and C. A. Balseiro, Phys. Rev. B **90**, 115423 (2014).
[45] P. M. Perez-Piskunow, L. E. F. Foa Torres, and G. Usaj, Phys. Rev. A **91**, 043625 (2015).
[46] M. Sentef, M. Claassen, A. Kemper, B. Moritz, T. Oka, J. Freericks, and T. Devereaux, Nature communications **6** (2015).
[47] J. Cayssol, B. Dóra, F. Simon, and R. Moessner, physica status solidi (RRL) Rapid Research Letters **7**, 101 (2013).
[48] Y. T. Katan and D. Podolsky, Phys. Rev. Lett. **110**, 016802 (2013).
[49] Y. Wang, H. Steinberg, P. Jarillo-Herrero, and N. Gedik, Science **342**, 453 (2013).
[50] Cf. J. Tong, J.-H. An, J. Gong, H.-G. Luo, and C. H. Oh, Phys. Rev. B **87**, 201109 (2013).
[51] A. G. Grushin, A. Gómez-León, and T. Neupert, Phys. Rev. Lett. **112**, 156801 (2014).
[52] C. He and Z. Zhang, Physics Letters A **378**, 3200 (2014).
[53] L. Zhou, H. Wang, D. Y. Ho, and J. Gong, The European Physical Journal B **87**, 204 (2014).
[54] E. Anisimovas, G. Žlabys, B. M. Anderson, G. Juzeliūnas, and A. Eckardt, Phys. Rev. B **91**, 245135 (2015).
[55] M. Benito and G. Platero, Physica E: Low-dimensional Systems and Nanostructures **74**, 608 (2015).
[56] A. Farrell and T. Pereg-Barnea, Phys. Rev. B **93**, 045121 (2016).
[57] L. Zhou, C. Chen, and J. Gong, Phys. Rev. B **94**, 075443 (2016).

[58] T.-S. Xiong, J. Gong, and J.-H. An, Phys. Rev. B **93**, 184306 (2016).
[59] K. Saha, Phys. Rev. B **94**, 081103 (2016).
[60] J.-i. Inoue and A. Tanaka, Phys. Rev. Lett. **105**, 017401 (2010).
[61] B. Dóra, J. Cayssol, F. Simon, and R. Moessner, Phys. Rev. Lett. **108**, 056602 (2012).
[62] N. H. Lindner, D. L. Bergman, G. Refael, and V. Galitski, Phys. Rev. B **87**, 235131 (2013).
[63] A. Kundu, H. A. Fertig, and B. Seradjeh, Phys. Rev. Lett. **113**, 236803 (2014).
[64] D. Y. H. Ho and J. Gong, Phys. Rev. Lett. **109**, 010601 (2012).
[65] H. Dehghani, T. Oka, and A. Mitra, Phys. Rev. B **90**, 195429 (2014).
[66] V. Dal Lago, M. Atala, and L. E. F. Foa Torres, Phys. Rev. A **92**, 023624 (2015).
[67] P. Titum, E. Berg, M. S. Rudner, G. Refael, and N. H. Lindner, Phys. Rev. X **6**, 021013 (2016).
[68] M. C. Rechtsman, J. M. Zeuner, Y. Plotnik, Y. Lumer, D. Podolsky, F. Dreisow, S. Nolte, M. Segev, and A. Szameit, Nature **496**, 196 (2013), letter.
[69] W. Zheng and H. Zhai, Phys. Rev. A **89**, 061603 (2014).
[70] M. D. Reichl and E. J. Mueller, Phys. Rev. A **89**, 063628 (2014).
[71] Z. Yan, B. Li, X. Yang, and S. Wan, Scientific Reports **5**, 16197 EP (2015), article.
[72] A. Verdeny and F. Mintert, Phys. Rev. A **92**, 063615 (2015).
[73] D. Leykam, M. C. Rechtsman, and Y. D. Chong, Phys. Rev. Lett. **117**, 013902 (2016).
[74] M. Račiūnas, G. Žlabys, A. Eckardt, and E. Anisimovas, Phys. Rev. A **93**, 043618 (2016).
[75] T. Kitagawa, E. Berg, M. Rudner, and E. Demler, Phys. Rev. B **82**, 235114 (2010).
[76] A. Gómez-León and G. Platero, Phys. Rev. Lett. **110**, 200403 (2013).
[77] M. S. Rudner, N. H. Lindner, E. Berg, and M. Levin, Phys. Rev. X **3**, 031005 (2013).
[78] D. Carpentier, P. Delplace, M. Fruchart, and K. Gawedzki, Phys. Rev. Lett. **114**, 106806 (2015).
[79] F. Nathan and M. S. Rudner, New Journal of Physics **17**, 125014 (2015).
[80] I. C. Fulga and M. Maksymenko, Phys. Rev. B **93**, 075405 (2016).
[81] M. Fruchart, Phys. Rev. B **93**, 115429 (2016).
[82] P. Leboeuf, J. Kurchan, M. Feingold, and D. P. Arovas, Phys. Rev. Lett. **65**, 3076 (1990).
[83] I. Dana, Phys. Rev. E **52**, 466 (1995).
[84] E. P. L. van Nieuwenburg, J. M. Edge, J. P. Dahlhaus, J. Tworzydło, and C. W. J. Beenakker, Phys. Rev. B **85**, 165131 (2012).
[85] R. W. Bomantara, G. N. Raghava, L. Zhou, and J. Gong, Phys. Rev. E **93**, 022209 (2016).
[86] M. Lababidi, I. I. Satija, and E. Zhao, Phys. Rev. Lett. **112**, 026805 (2014).
[87] H. Wang, D. Y. H. Ho, W. Lawton, J. Wang, and J. Gong, Phys. Rev. E **88**, 052920 (2013).
[88] M. Thakurathi, A. A. Patel, D. Sen, and A. Dutta, Phys. Rev. B **88**, 155133 (2013).
[89] D. Babajanov, D. U. Matrasulov, and R. Egger, The European Physical Journal B **87**, 258 (2014).
[90] S. Dasgupta, U. Bhattacharya, and A. Dutta, Phys. Rev. E **91**, 052129 (2015).
[91] A. Agarwala, U. Bhattacharya, A. Dutta, and D. Sen, Phys. Rev. B **93**, 174301 (2016).
[92] H. Huang, Z. Liu, H. Zhang, W. Duan, and D. Vanderbilt, Phys. Rev. B **92**, 161115 (2015).
[93] Z. F. Wang, Z. Liu, and F. Liu, Phys. Rev. Lett. **110**, 196801 (2013).
[94] D. Culcer, A. MacDonald, and Q. Niu, Phys. Rev. B **68**, 045327 (2003).
[95] J. Jung, A. M. DaSilva, A. H. MacDonald, and S. Adam, Nature Communications **6**, 6308 EP (2015), article.
[96] C. Ortix, L. Yang, and J. van den Brink, Phys. Rev. B **86**, 081405 (2012).
[97] M. Weinberg, C. Staarmann, C. lschlger, J. Simonet, and K. Sengstock, 2D Materials **3**, 024005 (2016).